Computational Analysis of Shear flow of Non-isothermal Rolie-poly Fluids

Mudau Ndamulelo (ndamulelo@aims.ac.za)

African Institute for Mathematical Sciences (AIMS)

Supervised by: Dr Tirivanhu Chinyoka
University of Cape Town, South Africa

26 October 2017

Submitted in partial fulfillment of a structured masters degree at AIMS South Africa

Abstract

The study of the shear flow in non-homogeneous Rolie-poly fluids is well-considered and frequently encountered in many industrial and technological applications such as extrusion of plastics, liquid metals, and polymer technology. The governing partial differential equations of momentum, temperature and Rolie-poly stresses used to describe the field flow are reviewed. The effect of various parameters such as Prandtl number, Reynolds number, Weissenberng number (reptation), Weissenberg number (Rouse) and convective-constraint release parameter on the velocity, temperature and Rolie-poly stresses profile are discussed. The partial differential equations governing the flow field have been solved numerically using finite difference method in case of semi-implicit and the obtained results are then discussed.

Keywords: Non-Newtonian fluids, Polymeric fluids, Non-isothermal, Shear-banding, Rolie-poly model, Viscoelastic, Finite difference.

Declaration

I, the undersigned, hereby declare that the work contained in this research project is my original work, and that any work done by others or by myself previously has been acknowledged and referenced accordingly.

Mudau.

Mudau Ndamulelo, 26 October 2017

Contents

1. Introduction

In the previous years a lot of work demonstrated shear-banding effects in complex fluids such as polymer melts and solutions. The expectation of shear-banding into the polymeric solutions is still difficult to be solved experimentally Li et al. (2013). But, theoretically, simple shear flow with bands is believed to origin from a constitutive instability (non-monotonic) in the deformation rate. For example such constitutive instabilities are studied possibly in wormlike micelles problem, where the loss of entanglements over flow-induced chain breakage is believed to produce a non-monotonic stress response Vasquez et al. (2007). For covalently bonded polymeric materials example, it is believed that the stress should increase monotonically with the increasing shear rate of the homogeneous fluid. This possibility would surely preclude shear-banding in polymeric materials, at least via a constitutive instability. In the next sections supporting key words to the present work are discussed in detail.

1.1 Fluids Rheology

Rheology is the study of deformation and flow of fluids in response to stress. To generate an incompressible fluid flow, a shear stress must be applied. Fluids include both gases and liquids. Here the focus is on the liquids Skelland (1967).

Consider a liquid confined between plates with area A as presented in (Fig.1.1). The top plate is moved constant velocity, U, by action of a shearing force F, although the bottom plate is fixed. In this context, the following definitions apply,
Shear stress: The shear stress, τ, is defined as the force per unit area F/A Skelland (1967).
Shear rate: If the variation in the velocity between the plates is constant, the shear rate, $\dot{\gamma}$, is the velocity difference between the plates divided by the distance between them, h Skelland (1967).
Viscosity: For a Newtonian the viscosity is defined by Newton's law of viscosity,

$$\tau = \eta\dot{\gamma} \tag{1.1.1}$$

The fluid viscosity η represent the resistance of the fluid to shearing force, and is called the dynamic viscosity Skelland (1967). The dynamic viscosity is defined as

$$\kappa = \frac{\eta}{\rho} \tag{1.1.2}$$

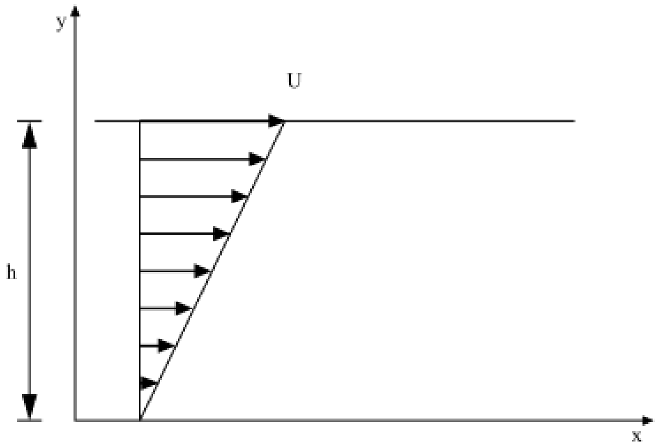

Figure 1.1: Schematic representation of one directional shearing flow Fielding (2017).

1.2 Classification Of Fluids

Fluids are typically classified into four categories, according to the relationship between the shear stress and shear rate:

1. Newtonian fluids.
2. Time-independent non-Newtonian fluids.
3. Time-dependent non-Newtonian fluids.
4. Viscoelastic fluids.

1.2.1 Newtonian Fluids. Newtonian fluids follow the simple rheological equation known as Newton's law of viscosity (Eq.1.1.1). The magnitude of the viscosity is not dependent on shear rate or time. Its rheological behavior (shear stress versus shear rate) is shown in (Fig. 1.2). It shows a linear relationship and passes through the origin. Water, vinegar, some motor oils and mineral oils are common Newtonian liquids Skelland (1967).

1.2.2 Time-Independent Non-Newtonian Fluids. Non-Newtonian fluids are only nature of fluid which do not obey Newton's law of viscosity (Eq.1.1.1). The shear stress is a non-linear function of the shear rate. (Fig.1.2) shows the rheological behavior of various types fluids. The viscosity of a time-independent non-Newtonian fluid is dependent on the shear rate Skelland (1967). Depending on how the apparent viscosity changes with shear rate the flow behavior is described as follows:

Shear thinning
The apparent viscosity of the fluid decreases with increasing shear rate. This type of behavior is also assigned to as 'pseudoplastic' and no initial stress (yield stress) is required to initiate shearing. A number of non-Newtonian materials are in this category, including grease,nail polish, whipped cream, molasses, paint, starch and many dilute polymer solutions Skelland (1967).
Shear thickening
The apparent viscosity of this fluid increases with increasing shear rate and no initial stress is required to initiate shearing. This type of behavior is also referred to as'dilatant'. A number of non-Newtonian materials in this category, including sand and water, peanut butter, corn and water are examples of dilatant liquids. Dilatant liquids are not as common as pseudoplastic liquids. Dilatant rheological

behavior is also shown in (Fig.1.2).
Viscoplastic Fluids Skelland (1967).
Viscoplastic materials are fluids that exhibit a yield stress. Under a certain critical shear stress there is no stable deformation of the fluid and it behaves like a rigid solid. When that shear stress value is exceeded, the material flows like a fluid. Bingham plastics are appropriate class of viscoplastic fluids that exhibit a linear behavior of shear stress versus shear rate before the fluid begins to flow. An example of a plastic fluid are toothpaste, die, mayonnaise, ketchup and puree, etc which will not flow out of the tube until a finite stress is applied by squeezing Skelland (1967).

1.2.3 Time-Dependent Non-Newtonian Fluids. For these types of fluids, their present behavior is determined by what happened to them in the recent past. These fluids seem to exhibit a 'memory' which fades with time. The apparent viscosity of the fluid depends on a number of properties including shear rate and the history of the shearing process. Depending on how the apparent viscosity changes with time the flow behavior is characterized as:

Thixotropic
A fluid is said to be thixotropic liquid when it decreases in the apparent viscosity over time at a constant shear rate. Once the shear stress is removed, the apparent viscosity starts increases and returns to its original value. When subjected to different rates of shear, a thixotropic fluid will shows a 'hysteresis loop'. Drilling mud, solder pastes, silca, honey, cytoplasm, inks and cement slurries are among the many materials which can exhibit thixotropic behavior Skelland (1967).
Rheopectic
A fluid is said to be rheopectic liquid if it exhibits a behavior opposite to that of a thixotropic liquid, i.e. the apparent viscosity of the liquid will increase over time at a constant shear rate. Once the shear stress is removed, the apparent viscosity starts decreases and returns to its original value. Rheopectic fluids are limited. Examples include specific gypsum pastes, cream, egg whites and printers inks Skelland (1967).

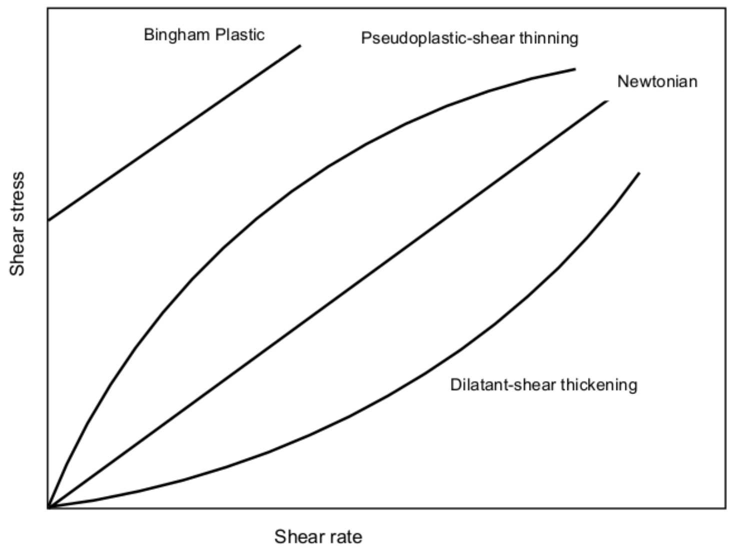

Figure 1.2: Rheological behavior of various types of non-Newtonian fluids Skelland (1967).

1.2.4 Viscoelastic Fluids. These materials exhibit both viscous (fluid-like) and elastic (solid-like) properties. The rheological properties of such a substance at any instant of time will be a function of the recent history of the material and cannot be described by simple relationships between shear stress and shear rate alone because the viscosity is not constant, but will also depend on the time derivatives of both of these quantities. Common examples of viscoelastic material are bread dough, oil, glycerine polymer melts and egg white Skelland (1967).

1.3 Polymeric Fluids

Polymeric fluids are the most important in complex fluids due to their rich rheological behaviour which determines the ease and expense of processing as well as the final properties of different manufactured products. Polymeric fluids are simple examples of 'viscoelastic' fluids Bird et al. (1987). The use of the word 'elastic' is to indicate the capability to restore its shape and original state after the release of the applied stress. Because of this property, polymeric fluids which have the elastic property are also known as 'memory' fluids.

Polymeric fluids generally show strong viscoelastic effects such as extension shear thickening, shear thinning, time-dependent rheology and viscoelastic normal stresses Larson (1999). In order to define the rheology of polymer liquids, systems of these materials under shearing or extensional flow are examined. There are many possible deformations that can be established on a polymeric fluid. Some of the simple geometries for imposing the shear flow, are parallel disks, sliding plates, concentric cylinders and the plate and cone Macosko (1994).

1.4 Non-isothermal Flow

By definition, nonisothermal flow refers to fluid flows with temperatures that are not constant. When a fluid is subjected to a temperature change, its material properties, such as density and viscosity, change accordingly.

So in polymeric flows another effect of great influence on the material properties, and thus on flow, is the temperature of the fluid. For polymeric fluids the shear and elongation viscosity are strong decaying functions of the temperature. Specially not far from the phase change of the the liquid to the solid state, this temperature dependence may be extremely large.

In addition, the temperature of polymeric fluids is changed by two ways. Firstly, temperature of a polymeric material in industrial processes is influenced by external heating (at the start of the production process) or cooling (at the end of the production process). However in the second case, during the deformation of polymeric fluids the temperature changes due to the internal energy production are also important. Due to the small thermal conductivity of polymer melts and concentrated polymeric solutions and the high viscosity the internal heat production is often not negligible Wapperom and Hulsen (1998).

1.5 Shear-banding

The development of shear-banding in the polymeric materials is an established problem in plastics and chemical engineering communities.

In 'shear-banding' phenomena, scientists have different explanations. For some non-Hookean solid materials, 'shear-banding' refers to the notion of strain localization. When a solid material is deformed, the strain can take large values in narrow zones of the sample. Similarly for some non-Newtonian fluids 'shear-banding' refers to the notion of strain rate localization. When the fluid is sheared, the strain rate can take large values in narrow zones of the sample. In both case, for solids or for fluids, shear-banding is linked to a sharp inhomogeneity in the deformation or deformation rate field Fardin (2012).

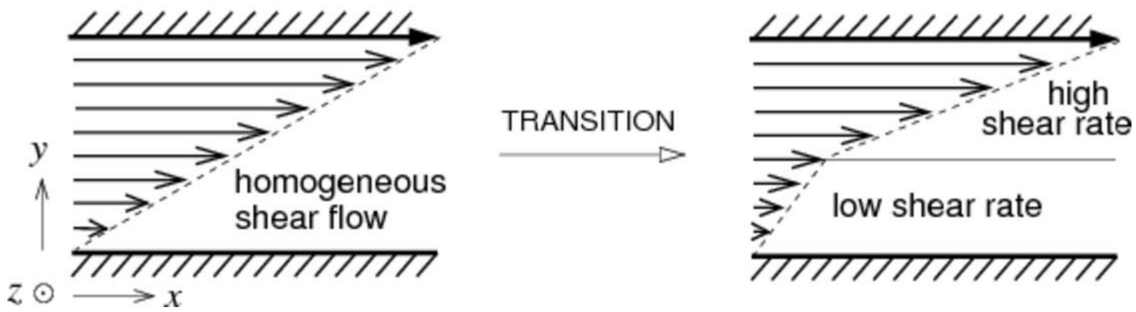

Figure 1.3: Schematic representation of one directional shear banding flow Fielding (2017).

1.6 Reynolds, Weissenberg and Prandtl Numbers

Reynolds number
The Reynolds number, R_e is a dimensionless number that used to describe fluid flows in classical Newtonian fluid dynamics, it is the ratio of inertial forces over viscous forces in a flow. A flow with a 'low' Reynolds number is more likely to be laminar as the viscous forces dominate the flow. However, a flow with a 'high' Reynolds number is more likely to be turbulent as the inertial forces dominate the flow. For an internal flow the Reynolds number is measured by employing features of the fluid (the viscosity and density), a length scale which arises from a characteristic fluid velocity and the geometry of the test rig Escudier (1998). The Reynolds number is generally described as

$$R_e = \frac{\rho u l}{\eta(\dot{\gamma})} \tag{1.6.1}$$

where u is the bulk velocity, ρ is the density, l is a characteristic length scale and η is the shear-viscosity.

Weissenberg number
The ratio of the microscopic time scale with the local strain rate is called the Weissenberg number:

$$W_i = \lambda\dot{\gamma} \quad \text{or} \quad \lambda\dot{\varepsilon} \tag{1.6.2}$$

where λ is the relaxation time and $\dot{\gamma}$ is the local strain rate.

In (Eq.1.6.2) the strain rate is the inverse of the kinematic scale. If the W_i is small, $Wi \ll 1$, it meaning that the elastic effects must negligible in the fluid flow. Most of the flow effects are seen around $\sim O(1)$. For a large W_i, $W_i \gg 1$, the liquid behaves almost like an elastic solid. The Weissenberg number is used only in the situations of a homogeneous stretching fluid packet in the flow. That is, the strain rates are uniform in space and time. Such a flow is encountered only in viscometric flows and theoretical analysis. Because is hard to experimented it into any practical application Samsal (1995).

Prandtl number

The Prandtl number is defined as the ratio of the molecular diffusivity of momentum to the molecular diffusivity of heat, ν/α Dewan et al. (2004).

2. Literature Review

In this chapter, a literature review on the shear flow instabilities problem will be presented. In fluid dynamics, if one knows the behaviour of the flow it is easy to check the instabilities using different constitutive models of non-Newtonian fluids and Naiver-Stokes equations. When the system contains nonlinear relationship between shear stress and strain rate, the coefficients will change the gradients. For example, in complex fluids the viscosity can not remain constant, but changes with the shear rate due to flow instabilities or any disturbance during the flow processes. To understand the behaviour of the flow instabilities various theories have been proposed.

Shear-banding predictions for two-fluid Rolie-poly model is investigated by Michael and Joseph (2016). In their work they experimented that shear flow solutions are used mainly to examine the details of the flow that developed from high Weinssenberg number instability and they also found out that the velocity and concentration distributions both exhibit important changes and structures for much lesser times. The shear-banding aspects in the entangled polymer systems was investigated in a planar couette cell with the Rolie-poly model by Changkwon and Chung (2011). In their detailed analysis they revealed that the difference of the broadness of the conformational bands and shear rate arises from competition of the molecular diffusion and relaxation mechanism affecting the conformational band. Therefore, their analysis was meaningful to understand the molecular level relaxation mechanism in the shear-banded system.

The theoretically study of the formation of shear bands in time-independent flows of polymeric and worm-like micelles surfactant fluids, concentrating on the protocols of step shear strain, shear stress, and shear start up studied experimental by Moorcroft et al. (2014). They found out that definite banding arises transiently in each of these protocols, even in fluids for which the basic constitutive curve of stress as a function of strain-rate is unbanded due to monotonically and steadily flowing state. In addition, the thermodynamic study of shear banding in polymer solutions was studied by Soroush and Germann (2016). They developed a new two-fluid model for semi-dilute entangled polymer solutions using the generalized bracket approach of non-equilibrium thermodynamics. In their work they used cylindrical couette flow to check the behaviour of the shear banding and in their conclusion they found out the the stress-induced migration is the response for shear-band formation and also the steady state solution is unique for various independent of the applied deformation history and initial conditions.

Many researchers have commonly investigated the shear bands instability that occurs on the shear flows using only Naiver-Stokes equations and Rolie-poly model. However, in this project we are going to study shear flows of entangled polymer solutions , modelled as a Rolie- poly fluid to understand the behaviour of shear-banding on the flow using the finite difference method with concentration solution which is based on the work of Cromer et al. (2013).

3. Problem Statement

3.1 Research Gap

According to the literature review many authors have tried to investigate the Rolie- Poly model mainly theoretical and experimental than computational. Implementing Rolie-Poly model is more complicated compared to the theoretical and experimental. However,in this project we are going to use the computational approach to check the behaviour of velocity, temperature and non-isothermal Rolie-Poly stresses .

3.2 Problem Statement

To investigate the behaviour of shear flow in non-isothermal Rolie-Poly fluids.

Non-dimensional governing equations

The governing statements of conservation of mass, momentum and energy equation which governs the polymeric flow are as follows:

$$\nabla \cdot \vec{v} = 0 \qquad \text{continuity equation} \tag{3.2.1}$$

$$R_e \left[\frac{\partial \vec{v}}{\partial t} (\vec{v} \cdot \nabla) \vec{v} \right] = -\nabla p + \beta \nabla^2 \vec{v} + \nabla \cdot \mathbf{T} \quad \text{momentum balance} \tag{3.2.2}$$

$$R_e P_r \left[\frac{\partial T}{\partial t} + (\vec{v} \cdot \nabla) T \right] = \nabla^2 T + P_e Q_D \qquad \text{energy equation} \tag{3.2.3}$$

where P_r is the Prandtl number, $\vec{v}$ is the velocity field, p is the pressure, $\beta = \eta_s / (\eta_s + \eta_p)$ is the viscosity ratio of the solvent viscosity (η_s) to the total the viscosity (η_p being the polymer viscosity), R_e is the Reynolds number, $P_e = R_e P_r$ and Q_d is the total stress tensor Reis and Wilson (2013).

Assumptions

- We assumed that the flow is incompressible.
- The pressure gradient is zero in the simple shear flow.
- Non-slip conditions in the flow.

Cartesian coordinates of continuity equation

$$\frac{\partial u}{\partial x} + \frac{\partial v}{\partial y} = 0 \tag{3.2.4}$$

$$\frac{\partial u}{\partial x} = 0 \tag{3.2.5}$$

Because the force depends on y and t, it means that all the physical variables depends only in y and t.

$$u = u(t, y) \tag{3.2.6}$$

Cartesian coordinates of momentum balance

$$(\vec{v} \cdot \nabla)\,\vec{v} = \begin{pmatrix} u\dfrac{\partial u}{\partial x} \end{pmatrix} \begin{pmatrix} u \\ 0 \end{pmatrix} = \begin{pmatrix} 0 \\ 0 \end{pmatrix} \tag{3.2.7}$$

by substituting (Eq.3.2.7) into (Eq.3.2.2) we get the following,

$$R_e \begin{pmatrix} \dfrac{\partial u}{\partial t} \\ \\ 0 \end{pmatrix} = -\underbrace{\begin{pmatrix} \dfrac{\partial p}{\partial x} \\ \\ \dfrac{\partial p}{\partial y} \end{pmatrix}}_{=0} + \beta \begin{pmatrix} \dfrac{\partial^2 u}{\partial y^2} \\ \\ 0 \end{pmatrix} + \begin{pmatrix} \dfrac{\partial \mathbf{T}_{xy}}{\partial y} \\ \\ \dfrac{\partial \mathbf{T}_{yy}}{\partial y} \end{pmatrix} \tag{3.2.8}$$

Then,

$$R_e \frac{\partial u}{\partial t} = \beta \frac{\partial^2 u}{\partial y^2} + \frac{\partial \mathbf{T}_{xy}}{\partial y} \tag{3.2.9}$$

Cartesian coordinates of energy equation

$$Q_D = (1-\gamma)\left[\beta\left(\frac{\partial u}{\partial y}\right)^2\right] + \gamma \mathbf{T}_{xy}\frac{\partial u}{\partial y} \tag{3.2.10}$$

By substituting (Eq. 3.2.10) into (Eq. 3.2.3) we get the following,

$$R_e P_r \frac{\partial T}{\partial t} = \frac{\partial^2 T}{\partial y^2} + P_e\left[(1-\gamma)\left[\beta\left(\frac{\partial u}{\partial y}\right)^2\right] + \gamma \mathbf{T}_{xy}\frac{\partial u}{\partial y}\right] \tag{3.2.11}$$

Initial and Boundary Conditions

We used (Fig.3.1) to construct the initial and boundary conditions of governing equations are as follows:

(i) For momentum equation

(Eq.3.2.4) is subjected to the following initial condition

$$\vec{u} = (u(t, y), 0, 0) = 0 \tag{3.2.12}$$

with boundary conditions (no slip)

$$u(t, 0) = 0, \qquad u(t, h) = u_0 \tag{3.2.13}$$

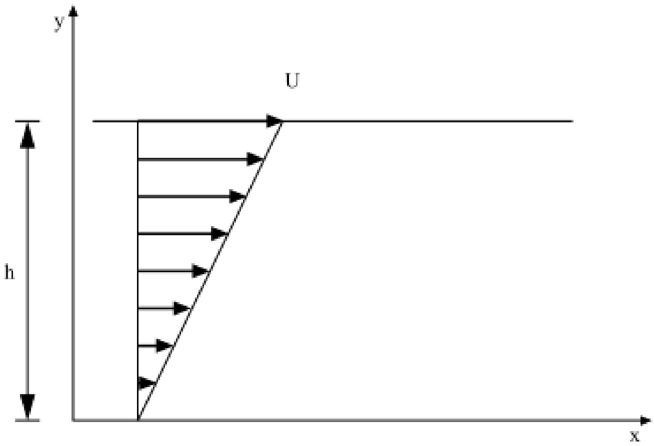

Figure 3.1: Schematic representation of one directional shearing flow Fielding (2017).

(ii) For energy equation

(Eq.3.2.11) is subjected to the following initial condition

$$T = T_0 \tag{3.2.14}$$

with boundary conditions

$$T(t, 0) = T_0, \qquad T(t, h) = T_0 \tag{3.2.15}$$

Viscoelastic constitutive equation

The Rolie-Poly constitutive equation for extra-stress Reis and Wilson (2013) may be written as:

$$\frac{\partial \mathbf{T}}{\partial t} + (u \cdot \nabla)\mathbf{T} - (\nabla u)\mathbf{T} - \mathbf{T}(\nabla u)^{\dagger} = -\frac{1}{\tau_d}(\mathbf{T} - \mathbf{I}) - \frac{2\left(1 - \sqrt{3/tr\mathbf{T}}\right)}{\tau_R}\left(\mathbf{T} + \beta^*\left(\frac{tr\mathbf{T}}{3}\right)^{\delta}\mathbf{T} - \mathbf{I}\right) \tag{3.2.16}$$

where τ_d is the Reptation time, τ_R is the Rouse relaxation time, β^* is the Convective-Constraint Release (CCR) parameter, $\mathbf{I}$ is the identity matrix, $\dagger$ denotes the matrix transpose, and tr denotes the trace of a tensor.

Then, the (Eq.3.2.16) into non- dimensionless state is given by:

$$W_e\left[\frac{\partial \mathbf{T}}{\partial t} + (u \cdot \nabla)\mathbf{T} - (\nabla u)\mathbf{T} - \mathbf{T}(\nabla u)^{\dagger}\right] = (1-\beta)\left(\nabla u + (\nabla u)^{\dagger}\right) - \mathbf{T}(1 + \frac{2W_e}{W_{eR}}) - \frac{2(1-\beta)}{W_{eR}}\mathbf{I}(1 - \sqrt{3/\sigma}) + \frac{2w_e\sqrt{3/\sigma}}{W_{eR}}\mathbf{T}(1-\beta^*) + \frac{6W_e\beta^*/\sigma}{W_{eR}}\mathbf{T} \tag{3.2.17}$$

Where W_e and W_{eR} are the Weissenberg numbers based on the Reptation time (τ_d) and Rouse time (τ_R), respectively, and

$$\sigma = \frac{W_e}{1-\beta}tr\mathbf{T} + trI \tag{3.2.18}$$

Now we rewrite (Eq.3.2.17) into matrix so that we can extract xx component, yy component and xy component of the Rolie-Poly stresses.

$$\left[\frac{\partial}{\partial t}\begin{bmatrix}\mathbf{T}_{xx} & \mathbf{T}_{xy}\\ \mathbf{T}_{xy} & \mathbf{T}_{yy}\end{bmatrix} - \begin{bmatrix}u\mathbf{T}_{xx} & u\mathbf{T}_{xy}\\ u\mathbf{T}_{xy} & u\mathbf{T}_{yy}\end{bmatrix} - \begin{bmatrix}\dot{\gamma}\mathbf{T}_{xy} & 0\\ \dot{\gamma}\mathbf{T}_{yy} & 0\end{bmatrix} - \begin{bmatrix}\dot{\gamma}\mathbf{T}_{xy} & \dot{\gamma}\dot{\gamma}\mathbf{T}_{yy}\\ 0 & 0\end{bmatrix}\right] = (1-\beta)\begin{bmatrix}0 & \frac{\partial u}{\partial y}\\ 0 & 0\end{bmatrix}$$
$$(1+\frac{2W_e}{W_{eR}})\begin{bmatrix}\mathbf{T}_{xx} & \mathbf{T}_{xy}\\ \mathbf{T}_{xy} & \mathbf{T}_{yy}\end{bmatrix} - \frac{2(1-\beta)}{W_{eR}}\begin{bmatrix}1 & 0\\ 0 & 1\end{bmatrix}\begin{bmatrix}1-\sqrt{3/\sigma} & 1-\sqrt{3/\sigma}\\ 1-\sqrt{3/\sigma} & 1-\sqrt{3/\sigma}\end{bmatrix} + \frac{2W_e\sqrt{3/\sigma}}{W_{eR}}\begin{bmatrix}\mathbf{T}_{xx} & \mathbf{T}_{xy}\\ \mathbf{T}_{xy} & \mathbf{T}_{yy}\end{bmatrix}$$
$$\begin{bmatrix}1-\beta^* & 1-\beta^*\\ 1-\beta^* & 1-\beta^*\end{bmatrix} + \frac{6W_e\beta^*\sigma}{W_{eR}}\begin{bmatrix}\mathbf{T}_{xx} & \mathbf{T}_{xy}\\ \mathbf{T}_{xy} & \mathbf{T}_{yy}\end{bmatrix} \tag{3.2.19}$$

where,

$$\begin{cases} C_1 = -\left(1+\frac{2W_e}{W_{eR}}\right) \\ C_2 = \left(\frac{2W_e}{W_{eR}}\sqrt{3/\sigma}\,(1-\beta^*)\right) \\ C_3 = \frac{6W_e\beta^*\sigma}{W_{eR}} \\ C_4 = -\frac{2(1-\beta)}{W_{eR}}\left(1-\sqrt{3/\sigma}\right) \end{cases}$$

Now by extracting xx component, yy component and xy component from (Eq.3.2.19) we get the following expression,

Rolie-Poly stresses in xy component

$$W_e\left(\frac{\partial \mathbf{T}_{xy}}{\partial t} - \mathbf{T}_{yy}\frac{\partial u}{\partial y}\right) = (1-\beta)\frac{\partial u}{\partial y} + (C_1+C_2+C_3)\,\mathbf{T}_{xy} \tag{3.2.20}$$

Rolie-Poly stresses in yy component

$$W_e\left(\frac{\partial \mathbf{T}_{yy}}{\partial t}\right) = (C_1+C_2+C_3)\,\mathbf{T}_{yy} + C_4$$
$$\mathbf{T}_{yy} = -\frac{C_4}{C_1+C_2+C_3} \tag{3.2.21}$$

Rolie-Poly stresses in xx component

$$W_e\left(\frac{\partial \mathbf{T}_{xx}}{\partial t} - 2\mathbf{T}_{xy}\frac{\partial u}{\partial y}\right) = (C_1+C_2+C_3)\,\mathbf{T}_{xx} + C_4 \tag{3.2.22}$$

Initial and boundary conditions of Rolie-Poly stresses

(Eq.3.2.20), (Eq.3.2.21) and (Eq.3.2.22) are subjected to the following initial conditions

$$\mathbf{T} = 0 \tag{3.2.23}$$

with boundary conditions

$$\frac{\partial \mathbf{T}}{\partial y}\Big|_{j=1}^{\text{forward}} = \frac{\partial \mathbf{T}}{\partial y}\Big|_{j=2}^{\text{forward}}$$
$$\frac{\partial \mathbf{T}}{\partial y}\Big|_{j=N-2}^{\text{forward}} = \frac{\partial \mathbf{T}}{\partial y}\Big|_{j=N-1}^{\text{forward}} \tag{3.2.24}$$

4. Methodology

In this chapter, We introduce the use of Computational fluid dynamics (CFD) followed by, the finite difference methods in detail.

Introduction and Motivation Of CFD

One of the benefits of using Computational Fluid Dynamics (CFD) is to find the optimized geometry and to understand the structures of the fluid flow, which is explained in theoretical fluid mechanics. As seen in relevant previous work, the simplifications and assumptions has been made to provide a suitable analytical solutions of fluid dynamics problems either Newtonian fluid problem or non-Newtonian fluid one. With today's advanced- technology, high- speed computing can be used to solve complex problems like non-Newtonian problems in fluid dynamics numerically Ferziger (2007). In order to do this, the Partial Differential Equations (PDEs) first have to be discretized to form a system of algebraic equations which can then be solved numerically. In this project, we have used one of the known Computational Fluid Dynamics approach (Finite Difference Method) to analyse the behaviour of shear-banding instability using Rolie-Poly model.

4.1 General Steps

To solve any computational fluid dynamics problem the following general steps are used.

1. The geometry (physical bounds) of the problem is characterized.
2. The problem domain is divided into discrete cells known as mesh or nodal network . The mesh can be uniform or non-uniform.
3. At boundary grid points, we employed the boundary conditions and substituted all derivatives in boundary conditions a by one sided finite difference approximations including values at interior nodes and boundary.
4. Then, we collected the algebraic conditions at entire grid point interior as well as boundary to obtained a system of algebraic equations in terms of unknown values of the variable at these nodes.
5. Finally, we solved the resulting equations in terms of unknown values of the variable at these nodes.

4.2 Partial Differential Equation

Partial Differential Equation (PDE) is a differential equation that consists the number of unknown multi-variable functions. A partial differential equation that involves the partial derivative shown in the previous in which u, T, T and p are treated as the function of y and t.

Partial differential equation are generally employed to build up a model of the most elemental theories underlying engineering and physics. Partial differential equation are employed to model the multidimensional systems. The governing equations and constitutive model with respect to time over a given region.

4.2.1 Numerical Methods. Two techniques are available to solve partial differential equations numerical way and analytical methods. Governing equations and constitutive problems with in-complex physical bounds are solved in analytical way but in reality the problem that contains the complex geometry together with complex boundary conditions which is not easier to solved analytically. In that fact high performance computers are implemented to get accurate approximate solution by using numerical Method.

In the numerical method, differential equations are replaced by the algebraic equations and for the 'n' unknown in the equations, 'n' algebraic equations are solved at the same time. Numerical formulation for the governing equations and constitutive equation can be obtained by finite difference method.

4.2.2 Finite Difference Method. In every numerical method, continuous partial differential equations are substituted by the discrete approximations Hoddmann and Chaing (2000). Here discrete conveys the context that solution is acknowledged only for definite number of points in the physical domain. These number of definite points in the domain is preferred by the programmer or user of the method. The increase in the number of discrete points in the domain increases the resolution and accuracy of the numerical solution.

The set of discrete points in the physical domain where discrete solution is known the mesh. The mentioned points are called nodes and if adjacent point are associated by the lines then the developing structure views related to the final or mesh $\Delta y, \Delta t$ are the main parameters in the mesh which are local distance among adjacent points in the space and local distance among the adjacent time steps.

In finite difference method, any derivative of partial differential equation is replaced by its truncated Taylor series expansion although equation is discretized term by term. Time derivative is linear

$$\frac{\partial u}{\partial t} = \frac{u(t+\Delta t) - u(t)}{\Delta t} \tag{4.2.1}$$

For spatial order derivative at least second order development is required to approach second-order derivatives

$$\frac{\partial^2 u}{\partial x^2} = \frac{u(x+\Delta x) - 2u(x) + u(x-\Delta x)}{(\Delta x)^2} \tag{4.2.2}$$

First order derivatives are commonly approximated by the backward and forward difference approximation

$$\frac{\partial u}{\partial x} = \frac{u(x+\Delta x) - u(x)}{\Delta x} \tag{4.2.3}$$

$$\frac{\partial u}{\partial x} = \frac{u(x) - u(x-\Delta x)}{\Delta x} \tag{4.2.4}$$

First order derivatives are commonly approximated by the central difference to avoid bias when choosing among backward difference and forward difference

$$\frac{\partial u}{\partial x} = \frac{u(x + \Delta x) + u(x - \Delta x)}{2\Delta x} \tag{4.2.5}$$

When a typical mesh is used, finite difference method generates the highly structured system of equations. The main advantage of finite difference method is the simple formulation of the method. Disadvantage is that, the finite difference method becomes complex in a non-rectangular geometries.

Finite difference method can be implemented in implicit or explicit manner, the latter is almost simple to set up and implement than the former. In case of the implicit approach, stability constraints over large values of time step developed in lesser computation time. Implicit method is more complicated to set up and program.

Finite difference method can also be implemented as semi-implicit method because it takes the average of the explicit and implicit method.

5. Implementation

5.1 Semi-Implicit Method

In this section we show how semi-implicit method is used to solve the governing equations and constitutive model called Rolie-Poly model.

(i) The finite difference equation of continuity equation in the semi - implicit formulation is:

$$\frac{\partial u^n}{\partial y} = \frac{u^n_{j+1} - u^n_{j-1}}{2\Delta y} = 0 \Rightarrow u^n_{j+1} = u^n_{j-1} \tag{5.1.1}$$

(ii) The finite difference equation of momentum balance in the semi - implicit formulation is:

$$R_e \frac{\partial u}{\partial t} = \beta \frac{\partial^2 u}{\partial y^2} + \frac{\partial \mathbf{T}_{xy}}{\partial y}$$

$$R_e \frac{u^{n+1}_j - u^n_j}{\Delta t} = \beta \frac{u^{n+1}_{j+1} - 2u^{n+1}_j + u^{n+1}_{j-1}}{(\Delta y)^2} + \frac{(\mathbf{T}_{xy})^n_{j+1} - (\mathbf{T}_{xy})^n_{j-1}}{2\Delta y} \tag{5.1.2}$$

(Eq.5.1.2) becomes,

$$-r_1 u^{n+1}_{j-1} + (R_e + 2r_1) u^{n+1}_j - r_1 u^{n+1}_{j+1} = R_e u^n_j + \frac{\Delta t}{2\Delta y}\left((\mathbf{T}_{xy})^n_{j+1} - (\mathbf{T}_{xy})^n_{j-1}\right) \tag{5.1.3}$$

where,

$$r_1 = \frac{\beta \Delta t}{\Delta y^2} \tag{5.1.4}$$

(iii) The finite difference equation of energy equation in the semi - implicit formulation is:

$$R_e P_r \frac{\partial T}{\partial t} = \frac{\partial^2 T}{\partial y^2} + P_e \left[(1-\gamma)\left[\beta\left(\frac{\partial u}{\partial y}\right)^2\right] + \gamma \mathbf{T}_{xy} \frac{\partial u}{\partial y}\right] \tag{5.1.5}$$

$$\frac{T^{n+1}_j - T^n_j}{\Delta t} = \frac{T^{n+1}_{j+1} - 2T^{n+1}_j + T^{n+1}_{j-1}}{(\Delta y)^2} + \frac{P_e}{4\Delta y^2}\beta(1-\gamma)(u^n_{j+1} - u^n_{j-1})^2 + \frac{P_e}{2\Delta y}(\mathbf{T}_{xy})^n_j (u^n_{j+1} - u^n_{j-1}) \tag{5.1.6}$$

By multiplying (Eq.5.1.6) with Δt it becomes,

$$\begin{aligned} -r_2 T^{n+1}_{j-1} + (P_e + 2r_2) T^{n+1}_j - r_2 T^{n+1}_{j+1} = P_e T^n_j + \frac{P_e}{4}\beta(1-\gamma) r_2 (u^n_{j+1} - u^n_{j-1})^2 \\ \frac{P_e}{2}\left(\frac{\Delta t}{\Delta y}\right)\gamma(\mathbf{T}_{xy})^n_j (u^n_{j+1} - u^n_{j-1}) \end{aligned} \tag{5.1.7}$$

where,

$$r_2 = \frac{\Delta t}{\Delta y^2} \tag{5.1.8}$$

(iv) The finite difference equation of Rolie-Poly stresses in xy component n the semi - implicit formulation is:

$$W_e\left(\frac{\partial \mathbf{T}_{xy}}{\partial t} - \mathbf{T}_{yy}\frac{\partial u}{\partial y}\right) = (1-\beta)\frac{\partial u}{\partial y} + (C_1+C_2+C_3)\,\mathbf{T}_{xy} \tag{5.1.9}$$

$$\begin{aligned} W_e\frac{(\mathbf{T}_{xy})_j^{n+1} - (\mathbf{T}_{xy})_j^n}{\Delta t} - (C_1+C_2+C_3)(\mathbf{T}_{xy})_j^{n+1} &= W_e(\mathbf{T}_{yy})_j^n\frac{(u_{j+1}^n - u_{j-1}^n)}{2\Delta y} \\ &\quad + (1-\beta)(\frac{u_{j+1}^n - u_{j-1}^n}{2\Delta y}) \end{aligned} \tag{5.1.10}$$

Then,

$$\left[W_e - \Delta t\,(C_1+C_2+C_3)\right](\mathbf{T}_{xy})_j^{n+1} = \frac{\Delta t}{2\Delta y}\left(u_{j+1}^n - u_{j-1}^n\right)\left[W_e(T_{yy})_j^n + 1 - \beta\right] \tag{5.1.11}$$

(v) The finite difference equation of Rolie-Poly stresses in yy component in the semi - implicit formulation is:

$$\mathbf{T}_{yy} = -\frac{C_4}{C_1+C_2+C_3} \tag{5.1.12}$$

$$(\mathbf{T}_{yy})_j^n = -\frac{C_4}{C_1+C_2+C_3} \tag{5.1.13}$$

(vi) The finite difference equation of Rolie-Poly stresses in xx component in the semi - implicit formulation is:

$$W_e\left(\frac{\partial \mathbf{T}_{xx}}{\partial t} - 2\mathbf{T}_{xy}\frac{\partial u}{\partial y}\right) = (C_1+C_2+C_3)\,\mathbf{T}_{xx} + C_4$$

$$W_e\frac{(\mathbf{T}_{xx})_j^{n+1} - (\mathbf{T}_{xx})_j^n}{\Delta t} - (C_1+C_2+C_3)(\mathbf{T}_{xx})_j^{n+1} = 2W_e(\mathbf{T}_{xy})_j^n(\frac{u_{j+1}^n - u_{j-1}^n}{2\Delta y}) + C_4 \tag{5.1.14}$$

Then,

$$\left[W_e - \Delta t(C_1+C_2+C_3)\right](\mathbf{T}_{xx})_j^{n+1} = W_e(\mathbf{T}_{xx})_j^n + W_e(\frac{\Delta t}{\Delta y})(\mathbf{T}_{xy})_j^n(u_{j+1}^n - u_{j-1}^n) + \Delta t C_4 \tag{5.1.15}$$

(vii) Forward scheme boundary for xy component Rolie-Poly stresses:

$$\left(\frac{\partial \mathbf{T}_{xy}}{\partial y}\right)_{j=1}^n = \left(\frac{\partial \mathbf{T}_{xy}}{\partial y}\right)_{j=2}^n \tag{5.1.16}$$

By using forward approximation into (Eq.5.1.16) we get the following

$$\begin{aligned}
\text{at j=1} \qquad & \text{at j=2} \\
\frac{(\mathbf{T}_{xy})^n_{j+1} - (\mathbf{T}_{xy})^n_j}{\Delta x} &= \frac{(\mathbf{T}_{xy})^n_{j+1} - (\mathbf{T}_{xy})^n_j}{\Delta y} \\
(\mathbf{T}_{xy})^n_2 - (\mathbf{T}_{xy})^n_1 &= (\mathbf{T}_{xy})^n_3 - (\mathbf{T}_{xy})^n_2 \\
(\mathbf{T}_{xy})^n_1 &= 2(\mathbf{T}_{xy})^n_2 - (\mathbf{T}_{xy})^n_3 \\
\vdots \qquad & \vdots \qquad \vdots \\
(\mathbf{T}_{xy})^n_N &= 2(\mathbf{T}_{xy})^n_{N-1} - (\mathbf{T}_{xy})^n_{N-2}
\end{aligned} \tag{5.1.17}$$

(viv) Forward scheme boundary for yy component Rolie-Poly stresses:

$$\left(\frac{\partial \mathbf{T}_{yy}}{\partial y}\right)^n_{j=1} = \left(\frac{\partial \mathbf{T}_{yy}}{\partial y}\right)^n_{j=2} \tag{5.1.18}$$

By using forward approximation into (Eq.5.1.18) we get the following

$$\begin{aligned}
\text{at j=1} \qquad & \text{at j=2} \\
\frac{(\mathbf{T}_{yy})^n_{j+1} - (\mathbf{T}_{yy})^n_j}{\Delta y} &= \frac{(\mathbf{T}_{yy})^n_{j+1} - (\mathbf{T}_{yy})^n_j}{\Delta y} \\
(\mathbf{T}_{yy})^n_2 - (\mathbf{T}_{yy})^n_1 &= (\mathbf{T}_{yy})^n_3 - (\mathbf{T}_{yy})^n_2 \\
(\mathbf{T}_{yy})^n_1 &= 2(\mathbf{T}_{yy})^n_2 - (\mathbf{T}_{yy})^n_3 \\
\vdots \qquad & \vdots \qquad \vdots \\
(\mathbf{T}_{yy})^n_N &= 2(\mathbf{T}_{yy})^n_{N-1} - (\mathbf{T}_{yy})^n_{N-2}
\end{aligned} \tag{5.1.19}$$

(vvv) Forward scheme boundary for xx component Rolie-Poly stresses:

$$\left(\frac{\partial \mathbf{T}_{xx}}{\partial y}\right)^n_{j=1} = \left(\frac{\partial \mathbf{T}_{xx}}{\partial y}\right)^n_{j=2} \tag{5.1.20}$$

By using forward approximation into (Eq.5.1.20) we get the following

$$\begin{aligned}
\text{at j=1} \qquad & \text{at j=2} \\
\frac{(\mathbf{T}_{xx})^n_{j+1} - (\mathbf{T}_{xx})^n_j}{\Delta y} &= \frac{(\mathbf{T}_{xx})^n_{j+1} - (\mathbf{T}_{xx})^n_j}{\Delta y} \\
(\mathbf{T}_{xx})^n_2 - (\mathbf{T}_{xx})^n_1 &= (\mathbf{T}_{xx})^n_3 - (\mathbf{T}_{xx})^n_2 \\
(\mathbf{T}_{xx})^n_1 &= 2(\mathbf{T}_{xx})^n_2 - (\mathbf{T}_{xx})^n_3 \\
\vdots \qquad & \vdots \qquad \vdots \\
(\mathbf{T}_{xx})^n_N &= 2(\mathbf{T}_{xx})^n_{N-1} - (\mathbf{T}_{xx})^n_{N-2}
\end{aligned} \tag{5.1.21}$$

6. Results and Discussion

Unless otherwise stated, we employ the parameter values:

$$R_e = 1, \quad W_e = 0.5, \quad W_{eR} = 1.2, \quad \beta = 0.5, \quad \beta^* = 0.01, \quad \gamma = 0.5, \quad dt = 0.01, \quad P_e = 1$$

These will be the default values in this work. In the succeeding graphics, if any of these parameter values is not explicitly mentioned, it will be understood that such parameters take on the default values.

Figure 6.1: Newtonian case when $W_e = 0$

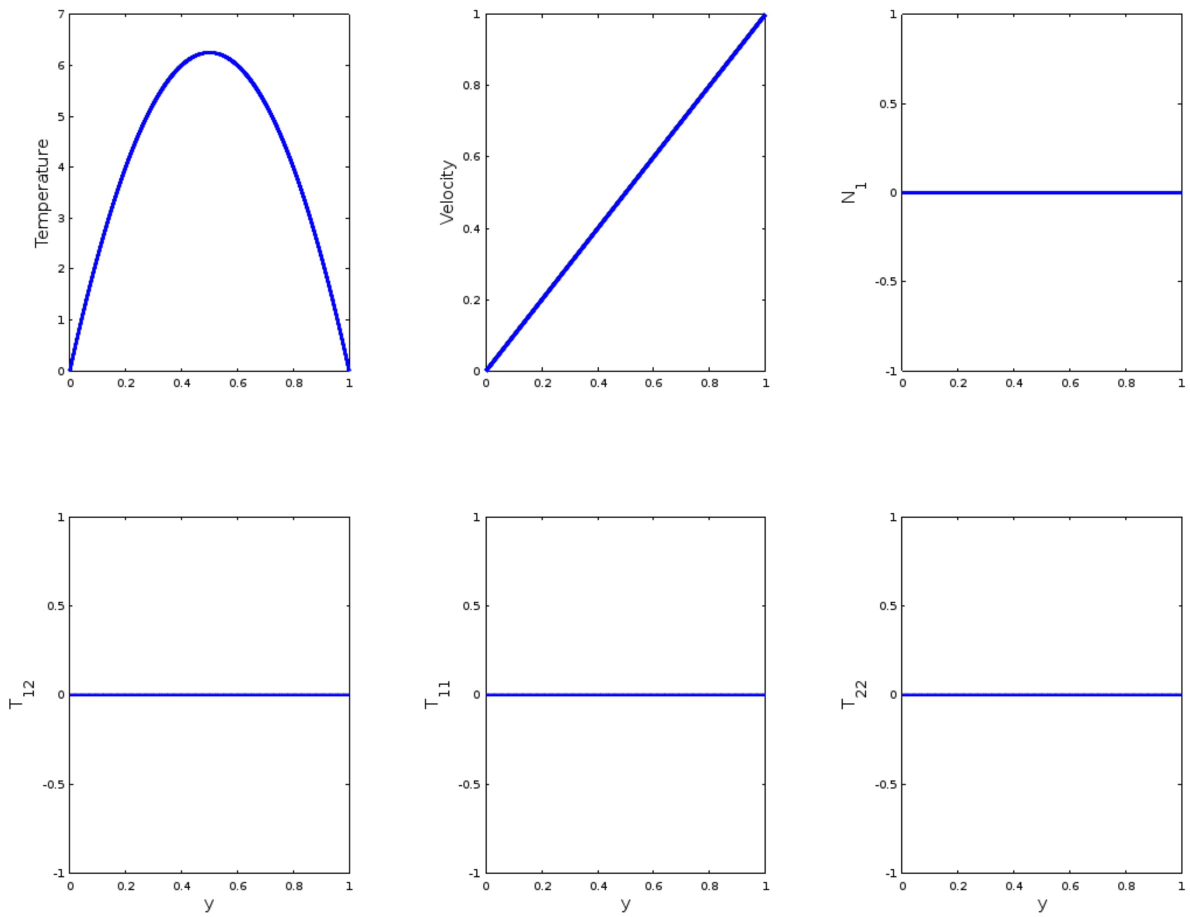

We display the solutions of Newtonian fluid when $W_e = 0$ in (Fig.6.1).

Figure 6.2: Non-Newtonian case when $W_e > 0$

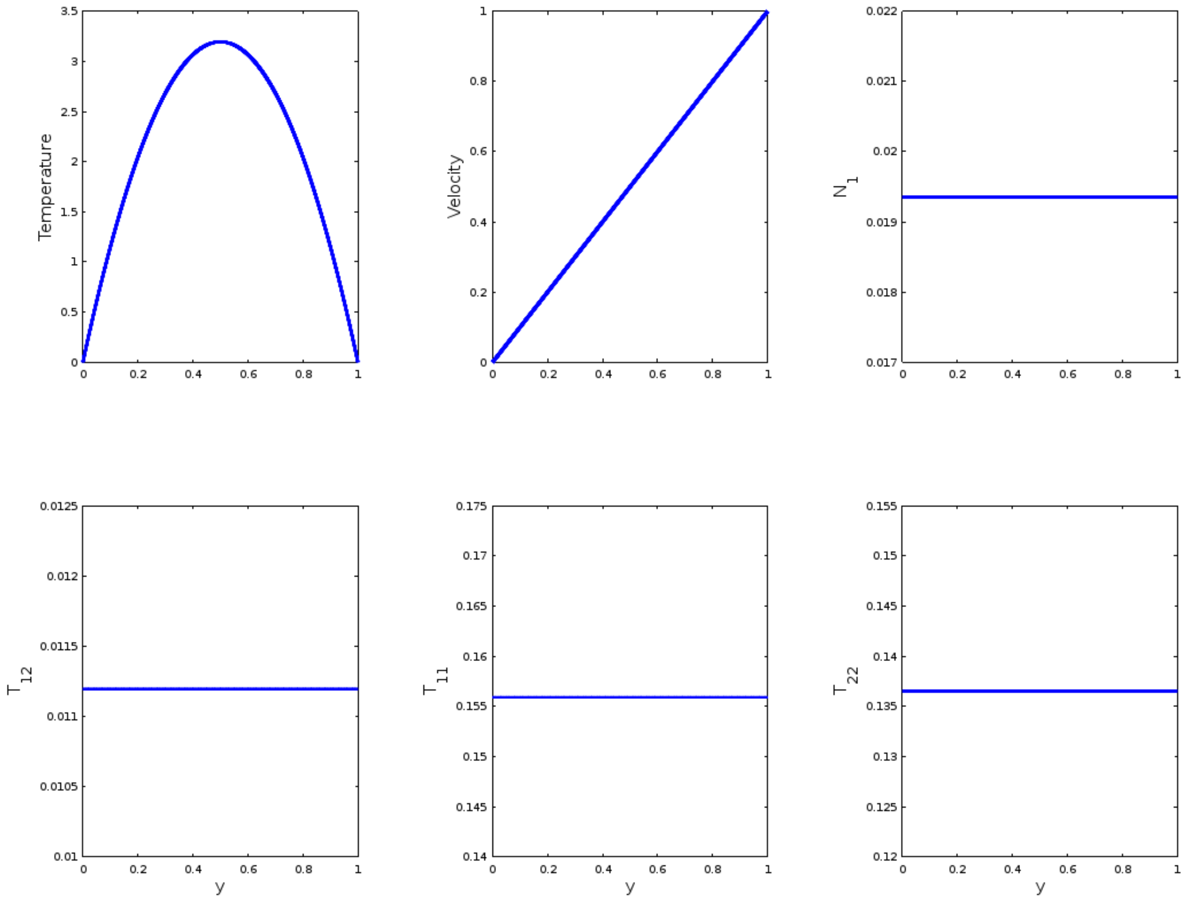

We also display the solution of viscoelastic quantities when $W_e > 0$ in (Fig. 6.2).

6.1 Parameter Depedence Solutions

The response of velocity, temperature and stresses into time development is illustrated in (Fig.6.3). We observed that as time increases the velocity and temperature profile reached the steady state. As expected, the stresses profiles becomes constant as time increases at the steady state case.

Figure 6.3: Time development of solutions to the steady state.

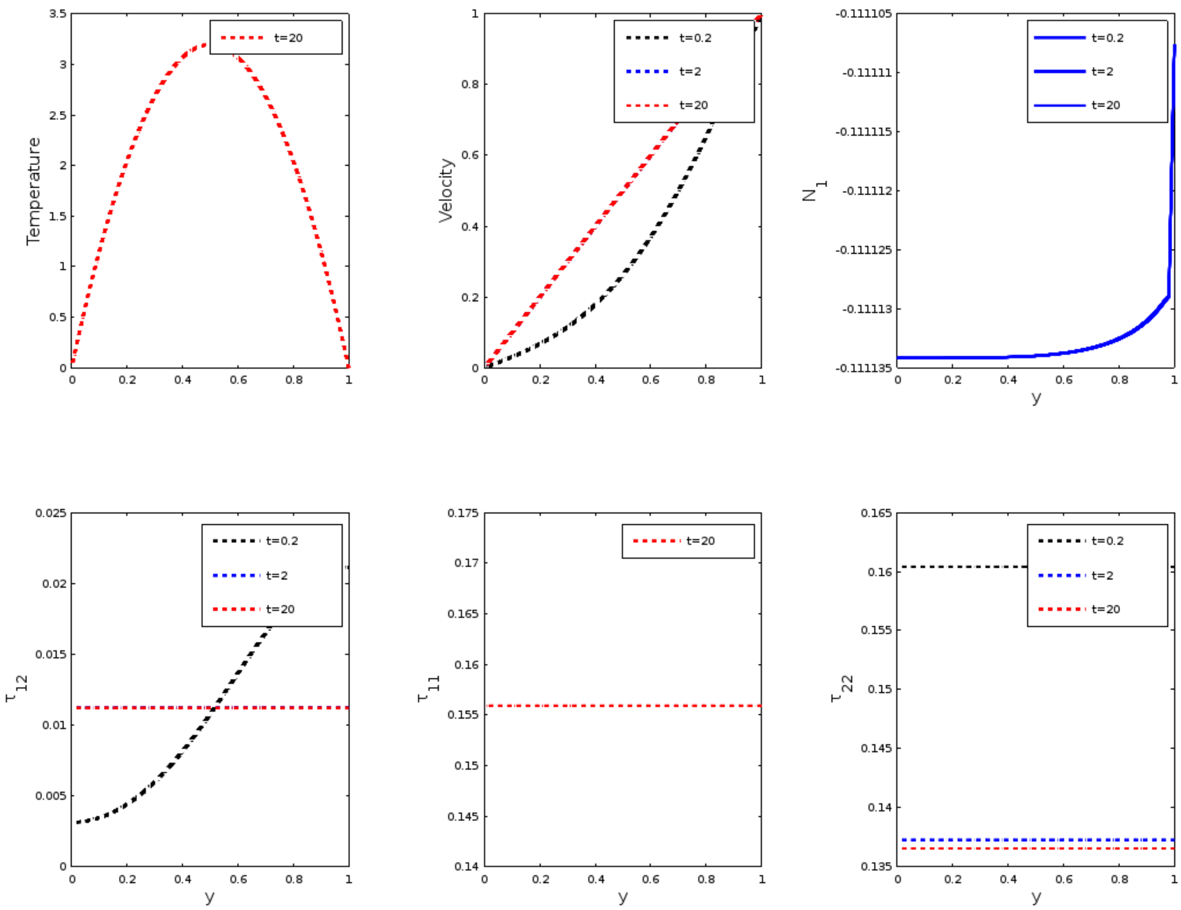

The response of velocity, temperature and stresses into Weissenberg number (Reptation) is illustrated in (Fig.6.4). We observed that the smaller the number of Weissenberg parameter (Reptation) the flow becomes more stable. On the other hand, we also observed that at larger Weissenberg number (Reptation), the instabilities rises as clearly showed in the $\mathbf{T}_{xx}$, $\mathbf{T}_{xy}$, $\mathbf{T}_{yy}$ and N_1 profiles. But on the velocity and temperature profiles, Weissenberg number (Reptation) has no effects.

Figure 6.4: Weissenberg number (Reptation) effects

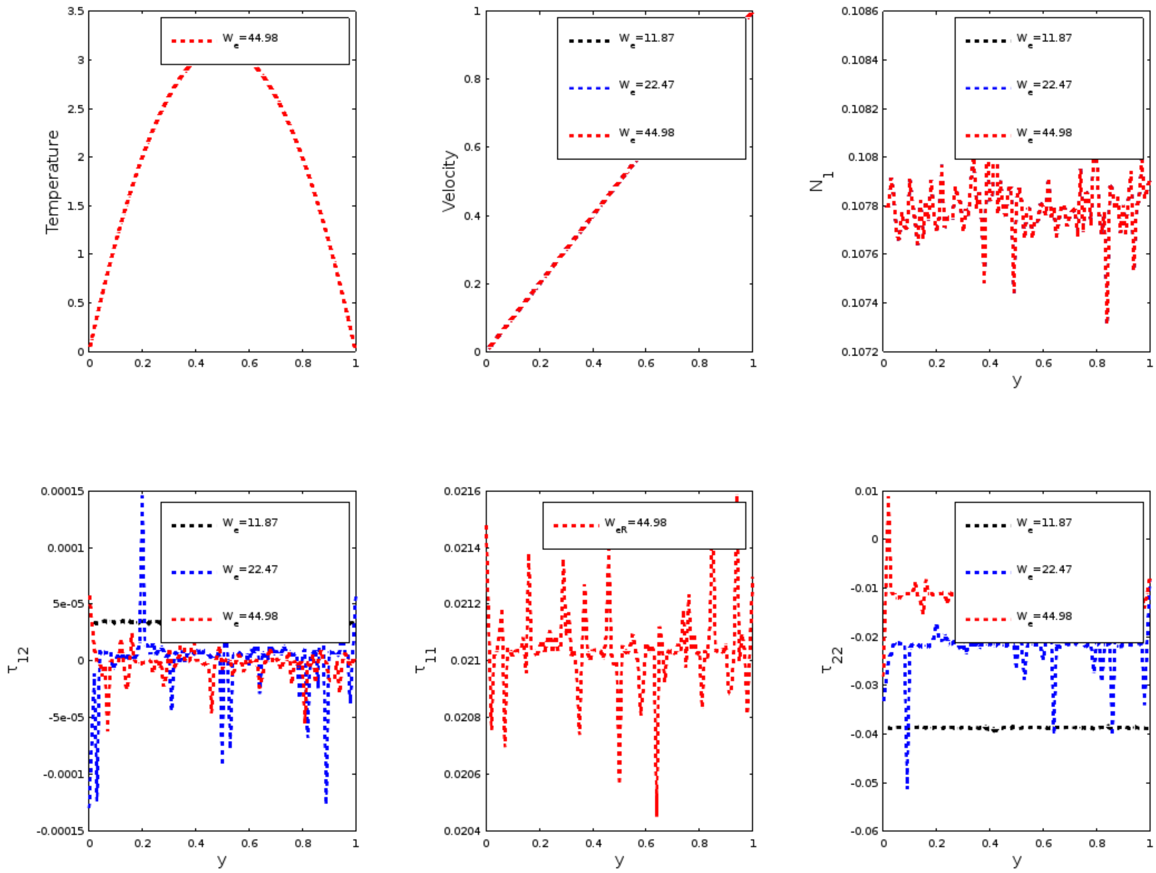

The response of velocity, temperature and stresses into Weissenberg number (Rouse) is illustrated in (Fig.6.5). On the profiles of $\mathbf{T}_{xx}$, $\mathbf{T}_{xy}$, $\mathbf{T}_{yy}$ and N_1, we observed that the smaller or larger the Weissenberg number (Rouse) does not affect the fluid flow. This suggest that the Weissenberg in polymeric materials exhibits the nature of stable than instability. But on the velocity and temperature profiles, Weissenberg number (Rouse) has no effects.

Figure 6.5: Weissenberg number (Rouse) effects

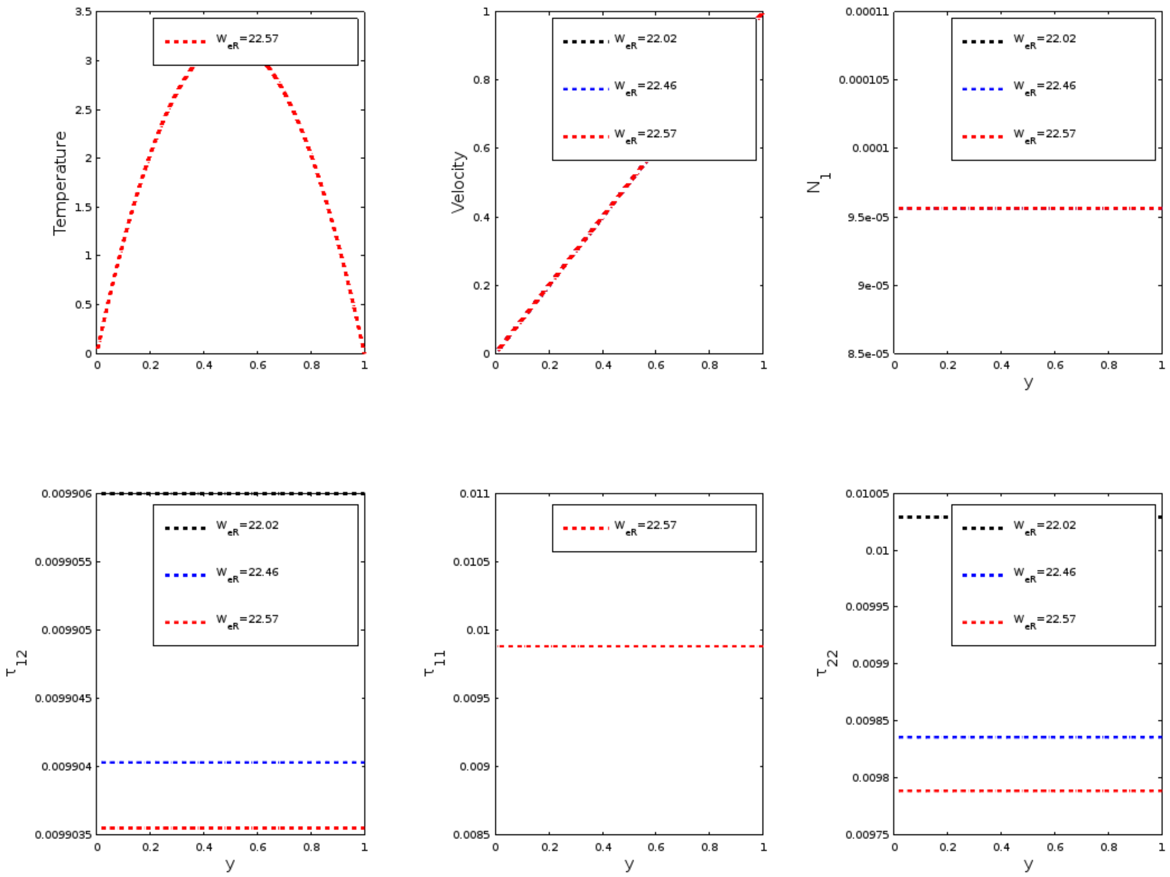

The response of velocity, temperature and stresses into Reynolds number is illustrated in (Fig.6.6). We observed that the larger the value of Reynolds number on velocity profile indicates that, the laminar layer of the fluid flow breaks-away and increases the displacement thickness all over the plate. On the other hand, we also observed that with the increase of Reynolds number the temperature profile move toward the outer wall. Because the material that contains high Reynolds number is hard to melts or heat it during industrial processes of polymeric substances. Finally, on the stresses we observed that as Reynolds number increases the stresses depicts exponential behaviour which indicates that the fluid flow is unstable.

Figure 6.6: Reynolds number effects

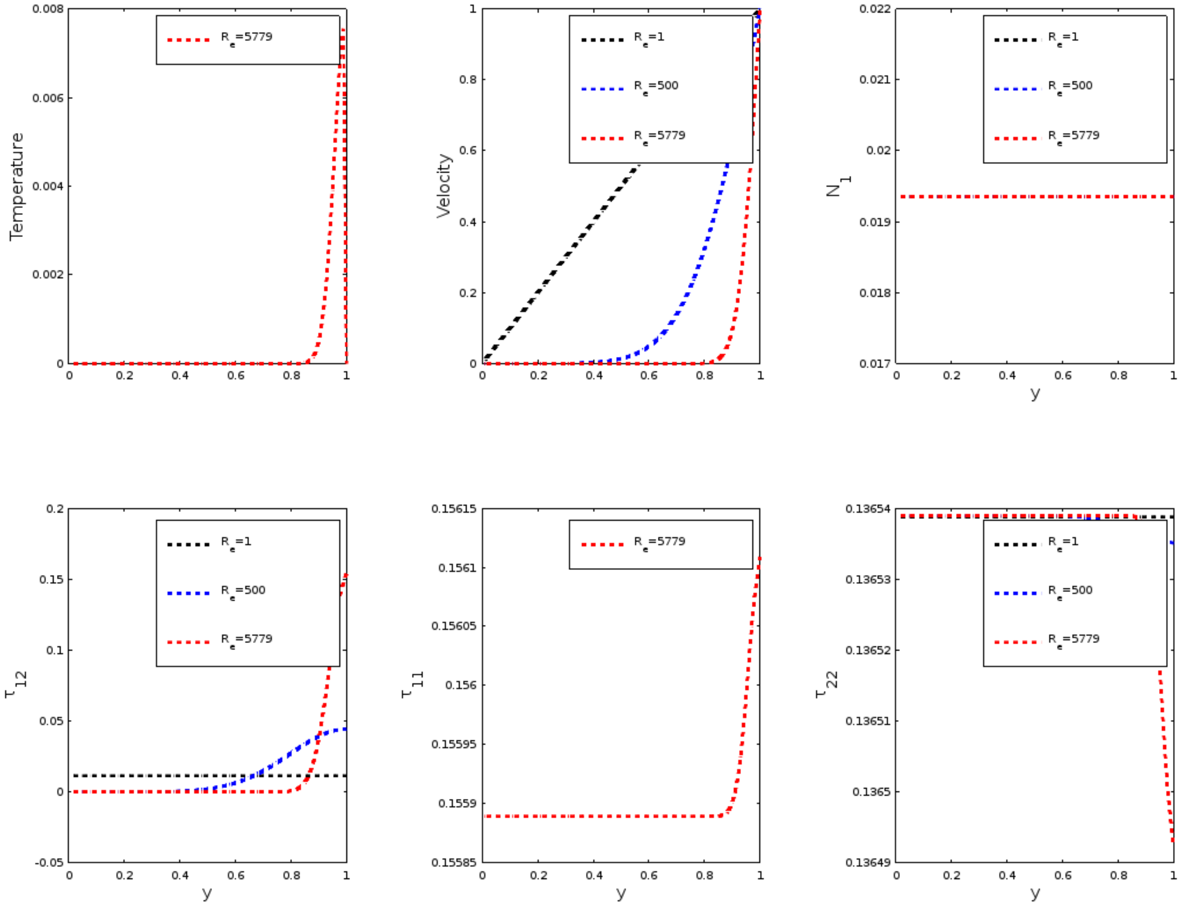

The response of velocity, temperature and stresses into Prandtl number is illustrated in (Fig.6.7). We observed that increase of Prandtl number decreases the temperature as shown in temperature profile. But on the velocity and stresses profiles Prandtl number has no effects.

Figure 6.7: Prandtl number effects

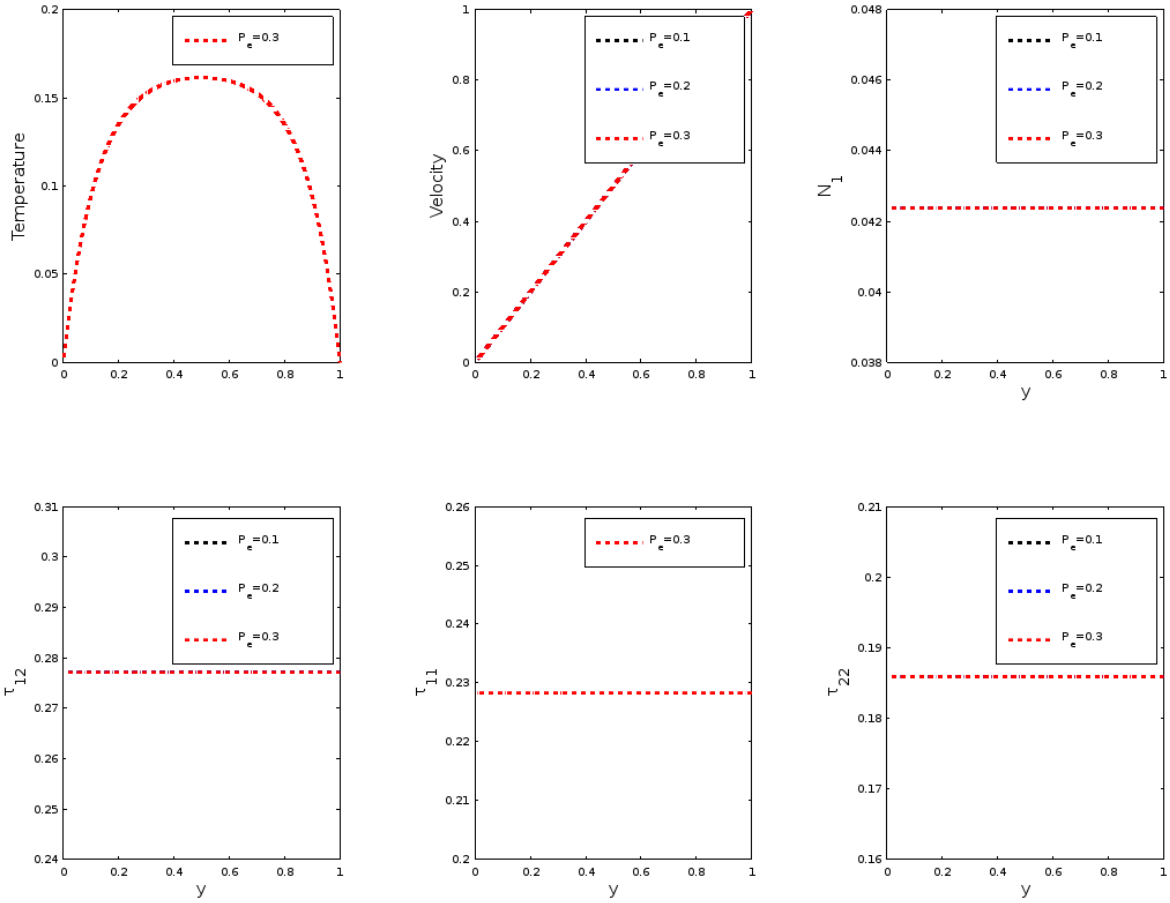

The response of velocity, temperature and stresses into viscosity parameter is illustrated in (Fig.6.8). We observed that increase in viscosity temperature rises. On the other hand of velocity profile, we observed that viscosity has no impact rather than measuring the resistance of the fluid flow. Finally, we also observed that as viscosity increases the stresses behave periodically which implies that the instability are there on the flow.

Figure 6.8: Viscosity effects

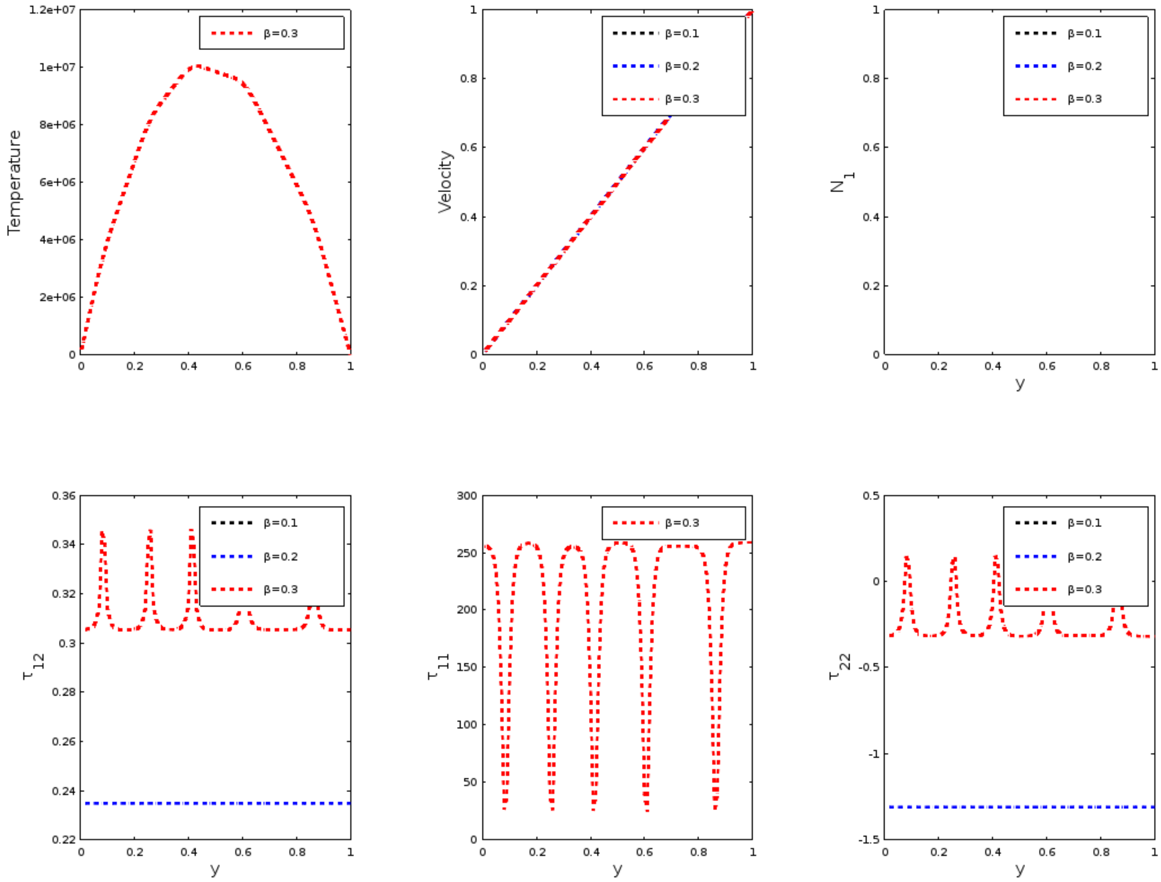

The response of velocity, temperature and stresses into viscosity parameter is illustrated in (Fig.6.9). We observed that increase the CCR parameter exhibits the nature of stable in the fluid flow. But on the velocity profiles, CCR parameter has no effects. Finally, we observed that temperature increases by increasing the CCR parameter.

Figure 6.9: CCR parameter effects

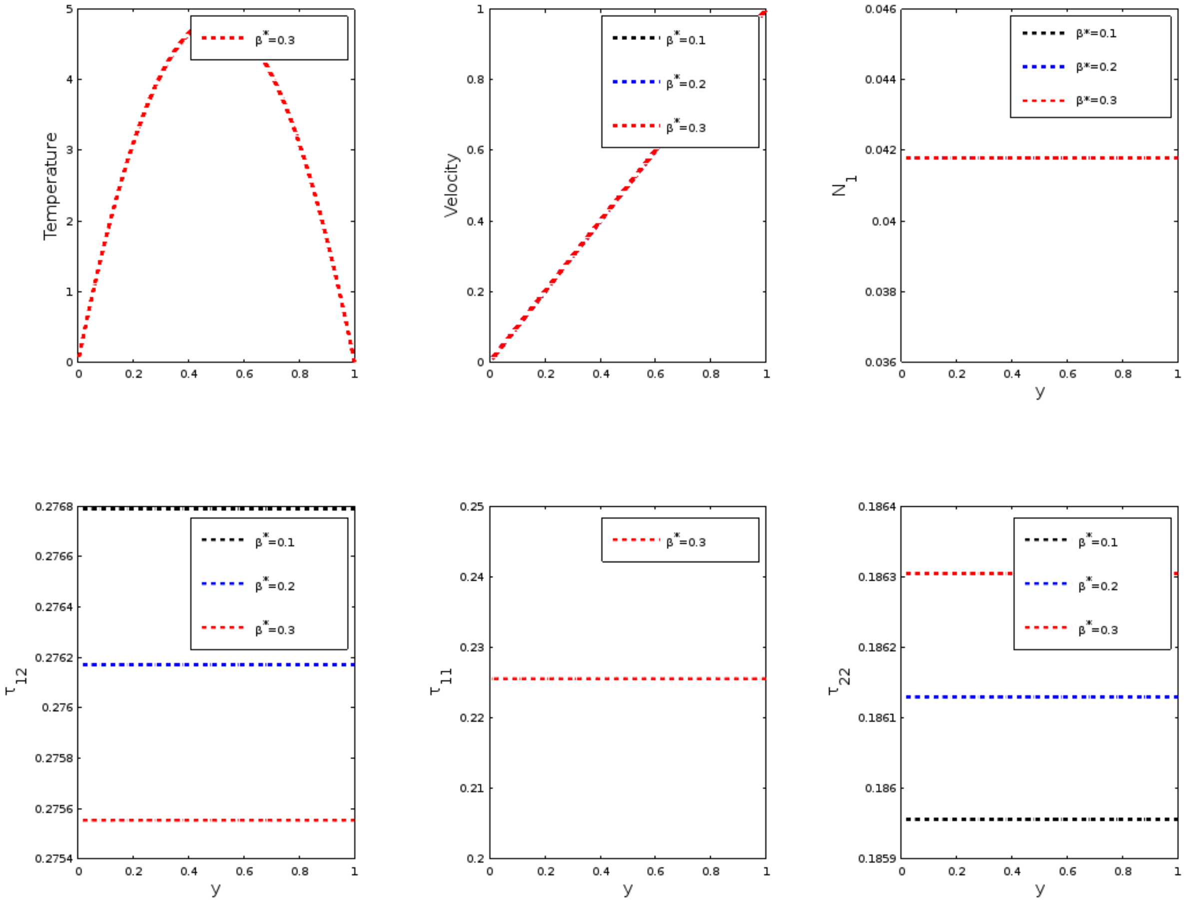

7. Conclusion

In this work, we analysed the shear flow of non-isothermal Rolie-poly fluids. The governing partial differential equations for mass, momentum and temperature used to describe the flow together with the constitutive equation called Rolie-poly model are reviewed. The resulting dimensionless partial differential equations are solved numerically by using finite difference method. The results for velocity, temperature, first normal-stress and Rolie-poly stresses profiles are studied and depicted graphically. The effects of Prandtl number, Weissenberg number (reptation relaxation time), Weissenberg number (Rouse relaxation time), convective-constraint release parameter, viscosity and Reynolds number on the velocity, temperature, first-normal stress and Rolie-poly stresses are studied. These results are particularly important for industrial purposes as they highlight the significance of shear flows that occur in the production of polymeric fluids.

7.1 Future Work

This work could be extended to check the behaviour of shear flow with the concentration solution.

Acknowledgements

I am grateful for the support and assistance of many people, which have allowed me to complete this research.

I would like to acknowledge the generous funding for this research provided by African Institute of Mathematical Sciences, without which this research would not have been possible.

I am also very thankful to my research supervisor Dr Tirivanhu Chinyoka, whose guidance and direction were essential to the completion of this research.

I would like to acknowledge the contribution and support from African Institute of Mathematical Sciences tutor for this research Mirette Fawzy.

Others thanks to my friends and colleagues at the African Institute of Mathematical Sciences, who have facilitated my transition to graduate studies and have helped make this experience pleasant.

Finally, I would like to thank my family for supporting and encouraging me throughout my studies.

References

B. Bird, C. R. Armstrong, and O. Hassager. Dynamics of polymeric liquids. *A Wiley-Interscience Publication, John Wiley and Sons*, 1, 1987.

C. Changkwon and Chung. Numerical study of chain conformation on shear banding using diffusive rolie-poly model. *Rheologica acta*, 50:754–766, 2011.

M. Cromer, L. Gary, and H. Glenn. Shear banding in polymer solutions. *Physics of Fluids*, 25, 2013.

A. Dewan, P. Mahanta, K. S. Raju, and P. S. Kumar. Review of passive heat transfer augmentation techniques. *Proceedings of the Institution of Mechanical Engineers, Part A: Journal of Power and Energy*, 218(7):509–527, 2004.

M. Escudier. *The essecence of Engineering Fluid Mechanics*. Prentice Hall Europe, 1998.

M. Fardin. *Soft Matter*, 8:910, 2012.

J. Ferziger. Computational methods for fluid dynamics. *Springer, Berlin, Germany*, 3, 2007.

S. Fielding. *http://community.dur.ac.uk/suzanne.fielding/interests.htmt*. 2017.

M. Graham. The sharskin instability of polymer melt flows. *Chaos 9*, 1:154–163, 1999.

K. Hoddmann and S. Chaing. *Computation Fluid Dynamics*. EES,Ch.02,03, 2000.

G. Larson. The structure and rheology of complex fluid. *Oxford university press*, 150, 1999.

Y. Li, B. McKenna, and L. Archer. Flow field visualization of entangled polybutadiene solutions under nonlinear viscoelastic flow conditions. *Journal of Rheology*, 57:411-1428, 2013.

C. W. Macosko. *Rheology: principles, measurements, and applications*. Wiley-vch, 1994.

P. Manjumadar. Computational methods for heat and mass transfer. *Taylor and Francis Group New York, Ny, USA*, 2005.

C. Michael and D. Joseph. Shear banding predictions for the two-fluid rolie-poly model. *Journal of Rheology*, 5:927–951, 2016.

L. Moorcroft, L. Robyn, and M. Fielding. Shear banding in time-dependent flows of polymers and wormlike micelles. *Journal of Rheology*, 58:103–147, 2014.

T. Reis and H. Wilson. Rolie-poly fluid flowing through constrictions. *Journal of Non-Newtonian fluid mechanics*, 195:77–87, 2013.

G. Samsal. A finite volume approach for calculation of viscoelastic flow through an abrupt axisymmetric contraction. *Journal of Non-Newtonian Fluid Mechanics*, 56:15-47, 1995.

A. H. P. Skelland. *Non-Newtonian flow and heat transfer*. Wiley, 1967.

H. Soroush and N. Germann. A thermodynamic study of shear banding in polymer solutions. *Physics of Fluids*, 28, 2016.

A. Vasquez, L. Cook, and G. McKinley. A network scission model for wormlike micellar solutions i: Model formulation and homogeneous flow predictions. *Journal of Non- Newtonian Fluid Mechanics*, 144:122-139, 2007.

P. Wapperom and M. A. Hulsen. Thermodynamics of viscoelastic fluids: the temperature equation. *Journal of Rheology*, 42(5):999–1019, 1998.